IT-SOFC supported on Mixed Oxygen Ionic-Electronic Conducting Composites

J. M. Serra,*[,†,‡] V. B. Vert,[‡] O. Büchler,[†] W. A. Meulenberg,[†] and H. P. Buchkremer[†]

Forschungszentrum Jülich GmbH, Institute for Materials and Processes in Energy Systems, IEF-1, D-52425 Jülich, Germany, and Instituto de Tecnología Química (UPV-CSIC), E-46022 Valencia, Spain

Received September 3, 2007. Revised Manuscript Received May 6, 2008

Thin oxygen-ion-conducting films (5−10 μm) were prepared and characterized on mixed-conducting porous substrates. When this film is made of a pure ionic conductor, such as a gadolinia-doped ceria ($Ce_{0.8}Gd_{0.2}O_{1.9}$) electrolyte material, the assembly can be used as a cathode-supported solid oxide fuel cell (SOFC) for operation at intermediate temperatures (500−600 °C). In this case, a porous anode comprising a Ni-CGO cermet or a Pt coating is deposited on top of the highly conductive electrolyte. Another structure with promising applications is created when the supported gastight layer includes a mixed conductor such as ferrite or cobaltite perovskites acting as oxygen-permeable membrane, which can be applied in the combustion of fuel with pure oxygen or in the intensification of other industrial processes currently using aerial catalytic oxidation. The different supported films and multilayer assemblies were characterized by SEM, EDS-WDX, SIMS, helium, and oxygen permeation, showing that gastight thin films can be achieved (values $>1 \times 10^{-6}$ mbar L s^{-1} cm^{-2}) by inexpensive coating procedures (screen-printing or slip-casting). The electrochemical properties of thin CGO electrolytes were studied by impedance spectroscopy (EIS) and DC voltammetry on fully assembled fuel cells. It is concluded that thin CGO electrolytes under hydrogen atmosphere have enough n-type electronic conductivity to reduce the cell potential by 5−20% from the Nernst potential, which causes the consequent power density decrease. A possible solution to these leakage currents is the use of a thin electron-blocking layer as stabilized zirconia (YSZ or SSZ) deposited on the fuel-exposed CGO electrolyte side. Oxygen permeation of thin LSFC layers was measured using air and helium (sweep) in the range from 700 to 1000 °C. Supported thin films exhibit much better permeation fluxes than bulk thick membranes, especially when oxygen-reduction catalytic porous coatings were applied.

1. Introduction

Solid oxide fuel cells (SOFC) are highly efficient energy converters, transforming the chemical energy directly into electrical power and a valuable hot stream. The development of an intermediate temperature SOFC (IT-SOFC)[1] would promote the introduction of this technology onto the market by reducing manufacturing costs and increasing their durability. To that end, very active electrocatalysts for both electrodes and thin highly conductive electrolytes are required. Typically, the thin electrolytes are supported on anode substrates (Ni-YSZ cermets) because these have appropriate mechanical and electrochemical properties. The present work reports on the use of cathode substrates based on mixed electronic-ionic conductors, as also recently discussed by Liu et al.[2]

The production of pure oxygen at high temperature through ceramic membranes would allow the introduction of more efficient and environmentally friendly power generation processes.[3–5] This is achieved in the oxyfuel process, where the fuel is combusted directly with pure oxygen (or enriched air) resulting in a flue gas essentially composed of wet CO_2, which can be readily separated. Oxygen-permeable membranes would benefit different chemical processes, allowing us to control the addition of oxygen through catalytic surfaces and potentially increasing the process selectivity. In addition, it would make process intensification possible[6,7] by reducing the presence of large amounts of nitrogen in the depleted gas stream.

Mixed ionic-electronic conducting perovskites and related structures are currently the most promising candidates for high-temperature oxygen-permeable membranes[8] and IT-SOFC cathodes.[9] The production of crack-free thin-films (thickness less than 25 μm) on tubular or planar geometries is extremely difficult. This issue was tackled by systemati-

* Corresponding author. Fax: 00340 963 877 809. E-mail: jsalfaro@itq.upv.es.
† Forschungszentrum Jülich GmbH, Institute for Materials and Processes in Energy Systems.
‡ Instituto de Tecnología Química.

(1) Hui, S.; Yang, D.; Wang, Z.; Yick, S.; Decès-Petit, C.; Au, W.; Tuck, A.; Maric, R.; Ghosh, D. *J. Power Sources* **2007**, *167*, 336.
(2) Liu, Y.; Hashimoto, S.; Nishino, H.; Takei, K.; Mori, M. *J. Power Sources* **2007**, *164*, 56.
(3) Wang, H.; Werth, S.; Schiestel, T.; Caro, J. *Angew. Chem., Int. Ed.* **2005**, *44*, 6906.
(4) Tan, X. Y.; Liu, Y. Y.; Li, K. *AIChE J.* **2005**, *51* (7), 1991.
(5) Sunarso J., Baumann S., Serra J. M., Meulenberg W. A., Liu S., Lin Y. S., Diniz da Costa J. C., *J. Membrane Sci.* **2008**, doi:10.1016/j.memsci.2008.03.074, available on-line April 15.
(6) Pérez-Ramírez, J.; Vigeland, B. *Angew. Chem., Int. Ed.* **2005**, *44*, 1112.
(7) Trunec, M.; Cihlar, J.; Diethelm, S.; Van Herle, S. *J. Am. Ceram. Soc.* **2006**, *89* (3), 955.
(8) Liu, Y. Y.; Tan, X. Y.; Li, K. *Catal. Rev. Sci. Eng.* **2006**, *48* (2), 145.
(9) Mai, A.; Haanappel, V. A.C.; Uhlenbruck, S.; Tietz, F.; Stöver, D. *Solid State Ionics* **2005**, *176*, 1341.

10.1021/cm702508f CCC: $40.75
Published on Web 05/30/2008

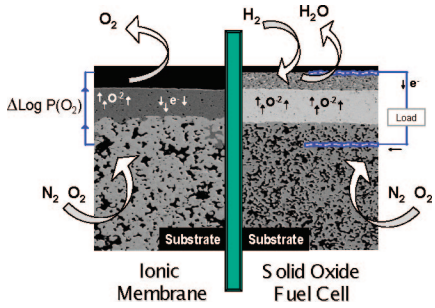

Figure 1. Schematic representation of the two proposed potential applications: (left) oxygen permeable membrane, where the dense thin-film comprises a mixed ionic-electronic conductor and the driving force for the separation is the gradient of oxygen partial pressure log $P(O_2)$; (right) solid oxide fuel cell, where the dense thin film comprises a nearly pure ionic conductor.

cally improving the substrate properties to fulfill requirements for obtaining crack- and pinhole-free thin layers. The variables modified in order to achieve appropriate substrate were[10] (i) composition, by using different mixtures of $La_{0.58}Sr_{0.4}Fe_{0.8}Co_{0.2}O_{3-\delta}$ (LSFC) and $Ce_{0.8}Gd_{0.2}O_{1.9}$ (CGO), (ii) the use of sintering additives, and (iii) the molding conditions (warm pressing), i.e., green density. The present paper describes the fabrication of thin oxygen-conducting gastight layers on these tailored mixed-conducting composites. The use of these supported films as IT-SOFC and also oxygen-permeable membranes is reported in detail. These two potential applications are outlined in Figure 1.

2. Experimental Section

2.1. Substrate Preparation. $Ce_{0.8}Gd_{0.2}O_{1.9}$ (CGO) was purchased from Treibacher (Austria). $La_{1-x}Sr_xCo_{1-y}Fe_yO_{3-\delta}$ ($y = 0$ and 0.8) perovskites were prepared by spray drying and finally fired at 900 °C for 5 h. The powders were examined by X-ray diffraction (XRD) to ensure phase purity and the exact composition was determined by ICP-AES. All the powders were preconditioned by ball milling in ethanol in order to achieve a mean particle size (d_{50}) of ~0.25 μm. The green substrates with dimensions of 70 × 70 × 2 mm^3 were fabricated by warm pressing (120 °C and 1 MPa) using a special coat-mix powder,[11,12] where the surfaces of the corresponding ceramic particles are coated with a phenol formaldehyde resin. This powder allowed high-porosity substrates to be produced, guaranteeing a fast gas exchange in high temperature asymmetric membranes and fuel cells. Further experimental details can be found in.[10] The substrates were thermally treated at 1100 °C in air to remove the binder and establish sufficient mechanical strength for further processing. Different substrate compositions were prepared by mixing CGO and LSFC and a sintering additive (Co_3O_4 produced by decomposition of cobalt nitrate). The combination of these two ionic conducting materials (CGO and LSFC) improved the manufacturing process, and both the final mechanical substrate properties and the electrochemical properties if the substrate was to act as a cathode. Moreover, an increase in the ionic conductivity has been described, with respect to the sole LSFC, when CGO was admixed.[13] The addition of CGO reduces LSFC coarsening and also the detrimental decrease in surface area resulting during the firing steps.

The presintered (at 1100 °C) porous substrates were subsequently coated by vacuum slip-casting or screen-printing in order to obtain the different thin (10−20 μm) oxygen-ion conducting top layers (CGO or LSFC). The slip and paste were prepared using powders with an average grain size of about 0.25 μm. Printing pastes were prepared by mixing equal amounts of ceramic powder and a solution (6 wt %) of ethylcellulose (Aldrich) in terpineol (Fluka). The coated substrates of 5 × 5 × 0.15 cm^3 were then sintered at 1200 °C for 3 h and the obtained layers were gastight and with a nearly flat top surface. The support shrinkage when raising from 1100 to 1200 °C represents an increase of ~45% in the substrate relative density, which is high enough to guarantee the densification of the coatings composed of CGO and LSFC/LSC nanosized grains.

In the case of supported CGO films (IT-SOFC electrolytes), three different porous coatings (electrodes) were applied by screen-printing on top of the sintered layer, in order to perform the different electrochemical measurements. For the EIS study, a top coating consisting of fine-grain LSFC was applied as counter electrode, whereas for the DC study, a top coating comprising either a CGO-NiO composite or a Pt paste were deposited. In all cases, the selected porous support consisted of a $La_{0.58}Sr_{0.4}CoO_{3-\delta}$-CGO (50:50 by weight percent) composite.

2.2. Characterization Techniques. The microstructure and the stability of the sintered layers were analyzed by SEM and EDS (Zeiss Ultra55 - INCAEnergy355 electron microscope) as well as by XRD at room temperature using a Siemens D500 diffractometer with Cu Kα radiation. Particle size was determined using a centrifugal analyzer (Shimazu, SA-CP3). The gas tightness of the supported films was checked by a helium leak test (helium leak detector quality test, Pfeiffer Vacuum GmbH). A sample is considered gastight if the leaking rate does not exceed 1 ×10^{-5} mbar L s^{-1} cm^{-2}. The depth element distributions of the films and membrane assembly were additionally determined by secondary ion mass spectrometry (SIMS; SIMSLAB 410 from Thermoquest), using a Ga primary ion source with fine focusing, a quadrupole mass spectrometer, postionization by electron beam, and duoplasmatron.

Electrochemical impedance spectroscopy (EIS) analysis was carried out using a disk-shaped sample 15 mm in diameter and a frequency response analyzer (Solartron 1260). The frequency range was 0.01 Hz to 4 MHz and the excitation amplitude was 3 mA. EIS measurements were carried out in air on a quasi-symmetric cell employing the following configuration: 1 mm thick $La_{0.58}Sr_{0.4}CoO_{3-\delta}$-CGO (50:50 by weight percent) porous support (acting as support and working electrode) ‖ 20 μm thick gastight CGO (acting as electrolyte) ‖ 25 μm thick porous LSFC (acting as counter electrode). This measurement was thought to electrochemically characterize the porous support and the electrolyte in oxidant conditions.

DC voltammetry was performed on a fully assembled cell having the following configuration: 1 mm thick $La_{0.58}Sr_{0.4}CoO_{3-\delta}$-CGO (50:50 by weight percent) porous support (acting as support and cathode) ‖ 20 μm thick gastight CGO (acting as electrolyte) ‖ 20 μm thick porous Pt layer (acting as anode). The top Pt coating was prepared by screen-printing a commercial Pt paste (Mateck, Germany) and subsequently sintering at 800 °C for 2 h. Moreover, an alternative anode layer comprising a CGO-Ni (50%-50% in vol.) composite was applied on the same support-electrolyte configuration. The electrochemical test was carried out on a CellTest 1470E

(10) Büchler, O.; Serra, J. M.; Meulenberg, W. A.; Sebold, D.; Buchkremer, H. P. *Solid State Ionics* **2007**, *178*, 91.
(11) Buchkremer, H. P.; Diekmann, U.; de Haart, L. G. J.; Kabs, H.; Stimming, U.; Stöver, D. *Proceedings of the 5th International Symposium on Solid Oxide Fuel Cells*, Achen, Germany, June 2, 1997; Electrochemical Society: Pennington, NJ, 1997; Vol. 97, p 160
(12) Dias F. J., Kampel M., Luhleich H. German Patents DE3305530 and DE3305529, to Forschungszentrum Jülich GmbH, 1984.
(13) Kharton, V. V.; Kovalevsky, A. V.; Viskup, A. P.; Shaula, A. L.; Figueiredo, F. M.; Naumovich, E. N.; Marques, F. M. B. *Solid State Ionics* **2006**, *160*, 247.

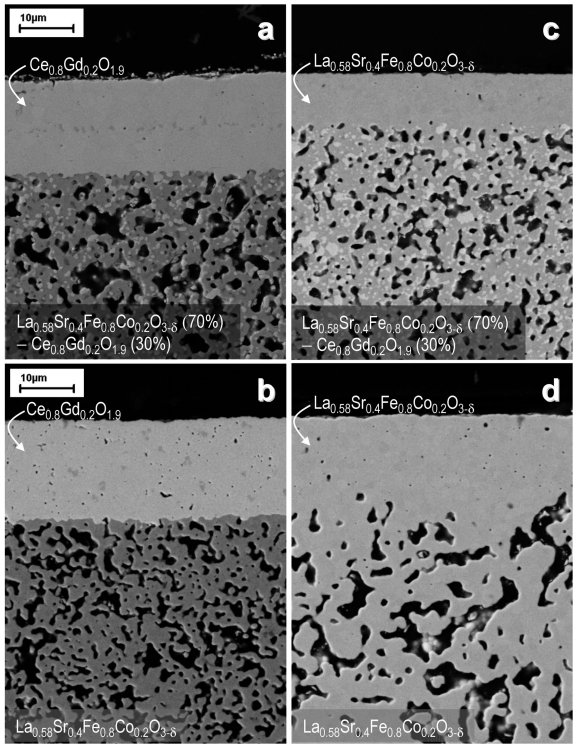

Figure 2. SEM pictures of gastight supported thin layers of CGO and LSFC on porous MIEC support comprising (a, c) mixtures of LSFC-CGO (70:30 ratio by weight percent) and (b, d) pure LSFC support. BSE detector shows the compositional contrasts, i.e., brighter zones correspond with CGO grains.

System (Solartron) coupled with two FRA modules (1455A). The cathode chamber was fed with synthetic air (300 mL/min) and the anode chamber was fed with hydrogen diluted with nitrogen (total flow 250 mL/min) to achieve three different H_2 concentrations, i.e., 2, 4, and 10%, and subsequently saturated with water at 25 °C. Lead (Pt) connections were done using Pt meshes on both cell sides and the cell was sealed using gold gaskets. Additionally, impedance measurements were carried out after recording the DC curve for each testing condition (temperature and % H_2). The thick $La_{0.58}Sr_{0.4}CoO_{3-\delta}$-CGO (50:50 by weight percent) support was selected for the electrochemical experiments for two reasons: (1) the higher content of CGO and consequently, the higher overall ionic conductivity of the support would be higher; and (2) the higher electronic conductivity of the LSC (see Figure S8 in the Supporting Information). Moreover, this support composition was one of the best formulations found[10] for the preparation of supported thin films.

Permeation measurements were performed on 15 mm diameter disks. This sample consisted of a gastight 10 μm thick LSFC layer supported on a LSFC-CGO (70:30 by weight percent) porous composite. The top surface of the LSFC was coated by screen printing with a 30 μm thick porous catalytic layer of $Pr_{0.58}Sr_{0.4}Fe_{0.8}Co_{0.2}O_{3-d}$ (1% Pd) for improving the surface oxygen exchange and sintered at 1040 °C. Sealing was done using gold gaskets in a setup similar to that outlined in ref 14. Oxygen was separated from synthetic air using 150 mL/min helium as the sweep gas and an MS analyzer (Balzers).

3. Results and Discussion

3.1. Microstructural Characterization. Figure 2a−d shows the two types of ion-conducting thin films prepared on two different substrates. First, pure ionic conducting films composed of CGO are presented in images a and b in Figure 2. These two CGO electrolytes have a thickness around 15 μm and are supported on two different substrates: (i) a composite (LSFC: CGO 70:30 wt/wt) substrate (Figure 2a); (ii) and a pure LSFC substrate (Figure 2b). In these images recorded with a back-scattered detector, it is possible to distinguish the compositional gradients; the bright layer/grains correspond in this case to CGO, whereas the dark ones are LSFC. The average grain size of the sintered (at 1200 °C) electrolyte was ~3 μm, as estimated from image analysis of SEM pictures at higher magnifications, while the starting paste or slip grain size was around 0.2 μm. The film in Figure 2a was deposited by screen-printing twice and therefore a few dark LSFC particles from the support can be observed in the former boundary between the two green printed CGO layers. On the other hand, the layer in Figure 2b was produced by slip-casting and in this case very few isolated LSFC particles are dispersed randomly within the electrolyte. Both techniques and both substrates are well-suited for the preparation of gastight thin CGO films, as stated by helium leak measurements. Phase purity (fluorite structure) of the CGO sintered layers was checked by XRD analysis carried out on the top surface.

On the other hand, mixed ionic and electronic conducting films composed of LSFC were prepared on the same two kinds of substrate and are shown in images c and d in Figure 2. These LSFC thin films have thicknesses of ~8 and 20 μm, respectively, whereas the average grain size for both is about 2 μm for both. No phase disaggregation is observed and only a few surface defects are observed although the layers are gastight.

After the final sintering, both kinds of supported thin layers, CGO and LSFC, show a high degree of densification, a flat top surface, and outstanding quality. This point was confirmed by helium leakage rate measurements of several layers, which exhibited rate values between 1×10^{-5} to 1×10^{-6} mbar L s^{-1} cm^{-2}. The samples have a typical geometry of $50 \times 50 \times 1$ mm^3 after the final firing step. The high quality and the low sintering temperature needed were achieved by carefully varying the substrate properties. Indeed, the effect of substrate composition (different $La_{0.58}Sr_{0.4}Fe_{1-x}Co_xO_{3-\delta}$-CGO proportions), the addition of cobalt oxide as CGO sintering enhancer, and the fabrication parameters (firing and pressing parameters) were studied. This thorough study[10] resulted in (i) improved shrinkage, specially in the range of 1100−1250 °C, where the densification process starts taking place for this kind of nanosized oxides; and (ii) matching of thermal expansion behavior, avoiding the formation of cracks during thermal cycling. Moreover, the most suited substrate compositions for the preparation of thin films found were: pure $La_{0.58}Sr_{0.4}Fe_{0.8}Co_{0.2}O_{3-\delta}$, composite $La_{0.58}Sr_{0.4}Fe_{0.8}Co_{0.2}O_{3-\delta}$-CGO (70:30 by weight percent) and $La_{0.58}Sr_{0.4}CoO_{3-\delta}$-CGO (50:50 by weight percent). Figure 3 shows the evolution of the substrate relative density as a function of the sintering temperature for these three substrate compositions. The CGO-containing substrates are preferred because of (i) the higher ionic conductivity;[13] (ii) improved mechanical properties and chemical stability; and (iii) flexibility of the fabrication method allowing better adjustment of the porosity. The low

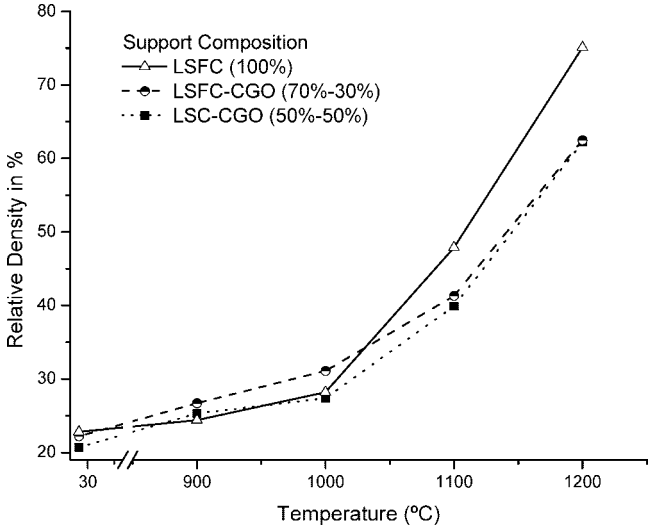

Figure 3. Evolution of the relative density of three different porous substrates as a function of the firing temperature.

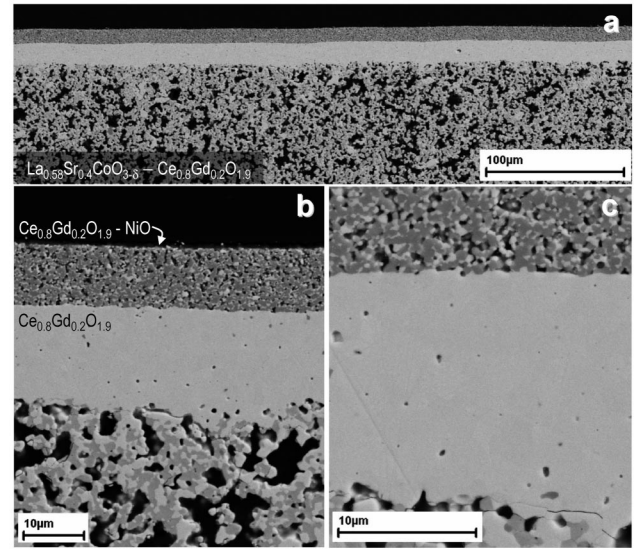

Figure 4. Cathode-supported fuel cell consisting of a LSFC-CGO cathode, a CGO electrolyte and a CGO-NiO anode (prior to reduction). The top anode was prepared by screen-printing a fine-grain CGO-NiO and subsequently sintered at 1100 °C in air. The different SEM images of polished cell cross-section show: (a) overview of the cell; (b) detail of the cathode (support)−electrolyte−anode interface; and (c) detail of the electrolyte microstructure, where 2 μm grains are visible.

firing temperature allowed a relatively high surface area to be retained in the porous substrate and adequate porosity for fast gaseous oxygen exchange, as assessed by air permeation measurements on uncoated substrates. In contrast, if a support with an unmatched thermal expansion coefficient is coated, as for a pure CGO substrate, then tensile cracks are formed during the cooling down period after sintering; however, the densification of the top layer is excellent because of the good support shrinkage behavior (from 1100 to 1200 °C). An example of these cracks can be observed in the LSFC layer on an all-CGO substrate in Figure S1 of the Supporting Information.

A fully assembled fuel cell was prepared by screen-printing a top anode layer comprising CGO and NiO on a CGO electrolyte supported on a LSC-CGO porous substrate and subsequently firing at 1100 °C for 3 h. Figure 4 shows SEM images of the cell cross-section in the oxidized state at three different magnifications. The quality and homogeneity of the CGO electrolyte and the fine-grained anode is visible in Figure 4a, whereas the fine anode microstructure and interface between the electrolyte and electrodes is more evident in images b and c in Figure 4. EDS-SEM analysis confirmed that the sintered layer contains the target CGO stoichiometry (see the Supporting Information). The anode composite is firmly attached to the electrolyte, which is also well-sintered with the substrate, as can been seen on the basis of the necking between CGO particles in that interface. The few microcracks present in the macroporous substrate are very likely produced during the preparation of the polished cross-section for SEM analysis.

Figure 5 shows the element distribution obtained by SIMS as a function of the depth for the cross-section of a half-cell consisting of a 10 μm thick CGO electrolyte supported on an all-LSFC substrate. This substrate composition was selected in order to better determine the cation diffusion and exchange between electrolyte and substrate. In this linescan, the sharp interface between electrolyte and substrate (for a linescan thickness of 200 nm) can be observed and thus no interdiffusion can be detected as a consequence of the relatively low sintering temperature required to achieve gas tightness. This is in agreement with the EDS analysis of several single points in the vicinity of the interface. Indeed, we observed that La and Co interdiffusion is a critical issue if the sintering temperature is raised above 1350 °C, as previously reported elsewhere.[15] Figure 6 presents the complete elemental mapping (SIMS) where electrolyte and substrate are clearly distinguished as in the SEM image of Figure 2a.

Figure 7 presents the elemental mapping obtained by EDS and WDS of a fracture section of a quasi-symmetric cell. This cell consists of a CGO electrolyte on a $La_{0.58}Sr_{0.4}CoO_{3-\delta}$-CGO (50:50 by weight percent) substrate, subsequently coated by screen printing with a 25 μm thick porous LSFC electrode and finally sintered at 1060 °C for 3 h. In the SEM (back-scattered electrons) image of Figure 7, the grain morphology can be seen, with average sizes ranging from 1 to 5 μm. The starting grain size (d_{50}) of the green-coated electrolyte was 0.2 μm; this size increases perceptibly during the sintering step, until it reaches values of 2−4 μm. This aspect is favorable, because very small particles, typically in the range of 50−200 nm, would produce an adverse increase in the electronic conductivity of the electrolyte, as described for instance in ref 16. Furthermore, the good attachment of the cathode support and the electrolyte, thanks to the good sintering of CGO grains from both layers, leads to the formation of highly conductive ionic paths. This interconnected three-dimensional CGO structure becomes readily visible in the Ce and Gd mapping of Figure 7. With respect to the top LSFC electrode, a fine porous structure ($d_{50} \approx 0.5$ μm) and good attachment to the electrolyte can

(14) Pérez-Ramírez, J.; Vigeland, B. *Catal. Today* **2005**, *105*, 436.
(15) Shaula, A. L.; Kharton, V. V.; Marques, F. M. B.; Kovalevsky, A. V.; Viskup, A. P.; Naumovich, E. N. *J. Solid State Electrochem.* **2006**, *10*, 28.
(16) Rupp, J. L. M.; Infortuna, A.; Gauckler, L. J. *Acta Mater.* **2006**, *54* (7), 1721.

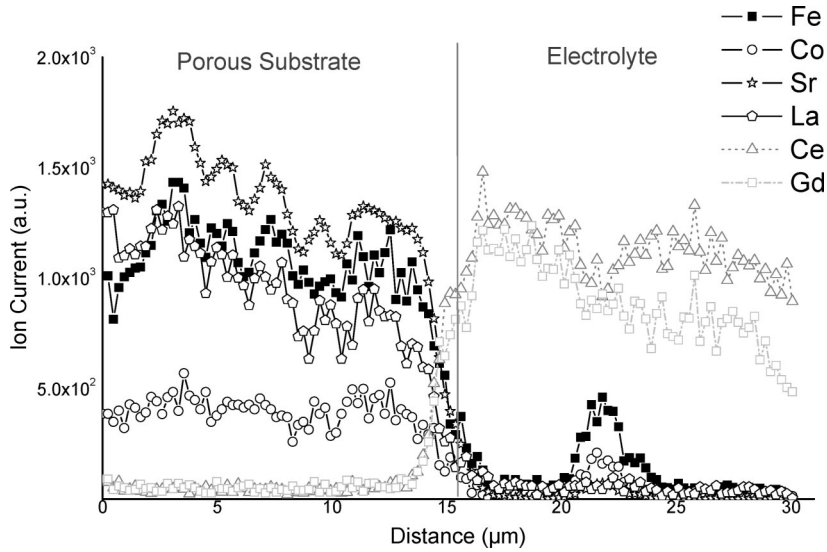

Figure 5. Qualitative depth profile analysis of elemental composition measured by SIMS for Ce, Gd, La, Sr, Fe, Co, and O. The sample consists of a 20 μm thick CGO electrolyte supported on a porous all-LSFC substrate and the analyzed zone corresponds to the electrolyte−substrate interface.

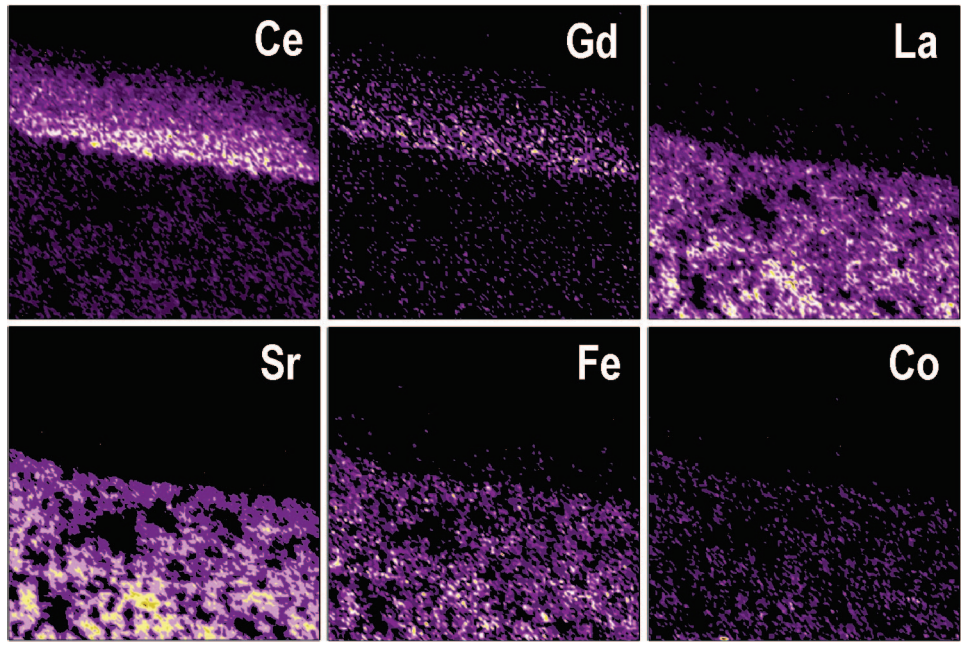

Figure 6. SIMS elemental mapping of the polished cross-section of the 20 μm thick CGO electrolyte supported on a porous all-LSFC substrate. Field of view 65.4 × 65.4 μm^2.

be observed. The three layers composing the assembly can be clearly recognized in the SEM (back-scattered electrons) and in the individual element mapping, confirming once again the absence of interdiffusion among the layers. However, sporadically, small cobalt oxide particles can be found in the substrate, which is ascribed to an excess of cobalt oxide added to the CGO as a sintering enhancer during substrate fabrication. Co is homogeneously distributed in the LSFC top coating and because of the smaller concentration (Fe/Co = 8/2), it is difficult to distinguish it in the comapping of Figure 7.

3.2. Electrochemical and Permeation Characterization. Figure 8 shows the Nyquist impedance plot recorded in air at three different temperatures for a thin CGO electrolyte supported on an LSC-CGO substrate and subsequently coated with a top LSFC electrode (quasi-symmetric cell). After the EIS measurement, the sample was analyzed by SEM corresponding to the sample in Figure 7. The impedance spectrum consists of three serial components, i.e., a pure resistance and two depressed semicircles in R(RQ)(RQ) configuration. The pure resistance is ascribed to the bulk electrolyte resistance of the oxygen ionic conduction whereas the grain boundary resistance is negligible, probably due to the large grain sizes compared to earlier studies with submicrometer grains.[17] The other two arcs at high (HF) and low frequency (LF) can be attributed to electrode polarization, which includes[18] catalytic oxygen reduction/oxidation, gas diffusion, ionic transport, and ion transfer between

(17) Zhou, X.-D.; Huebner, W.; Kosacki, I.; Anderson, H. U. *J. Am. Ceram. Soc.* **2002**, *85* (7), 1757.

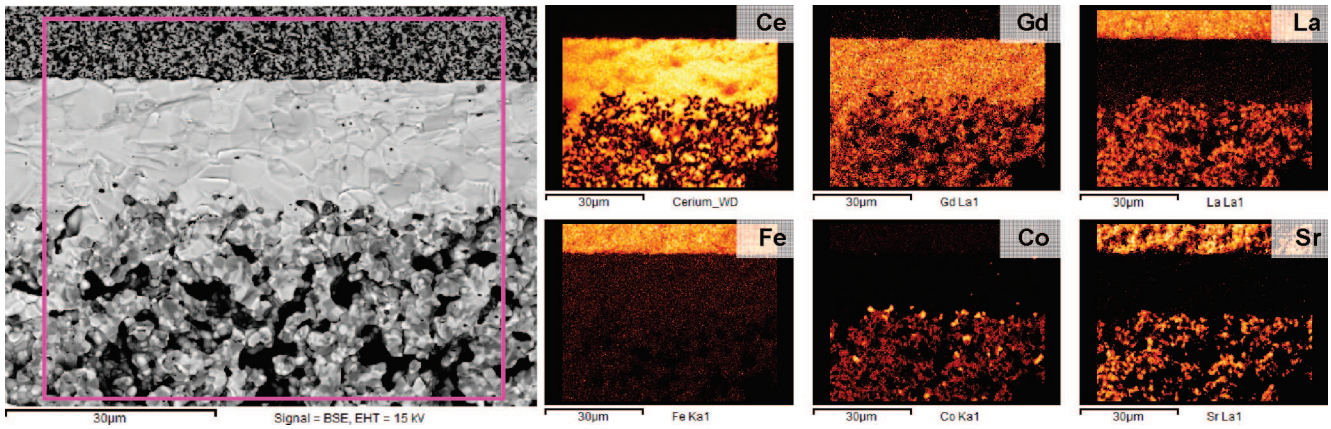

Figure 7. Microstructure and element distribution of cross-section of the quasi-symmetric cell for impedance measurement. This cell comprises a LSC-CGO porous substrate (WE), a 20 μm thick CGO electrolyte and a top porous LSFC counter electrode. (WDS employed uniquely for Ce determination): (left) BSE-detector micrograph, and (right) EDX and WDS elemental mapping of a fracture cross-section (WDS employed uniquely for Ce determination).

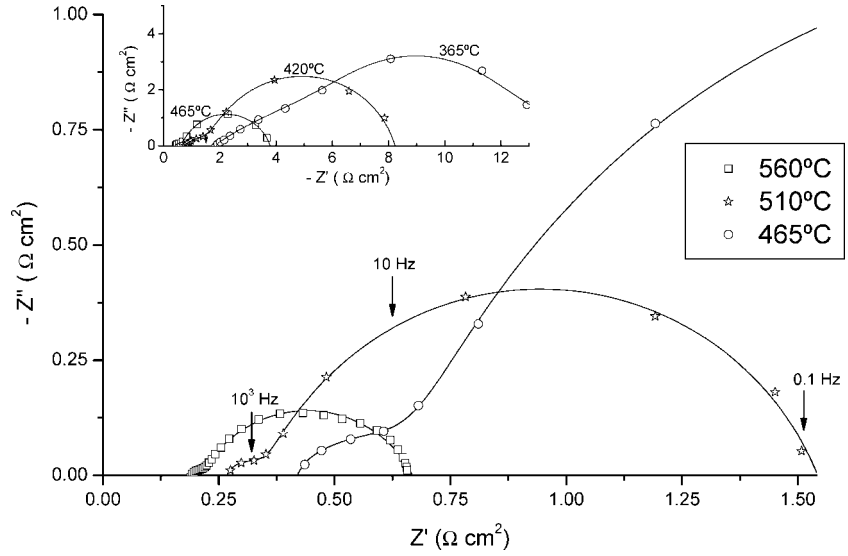

Figure 8. Nyquist impedance plots for the quasi-symmetric cell composed of (i) LSC-CGO (50:50 by weight percent) porous substrate (WE); (ii) a 20 μm thick CGO electrolyte; and (iii) a LSFC counter electrode: Variation of the temperature in air. Solid lines correspond to the fitted equivalent circuit response. Inset shows the spectra corresponding to the three lowest temperatures.

electrodes and electrolyte. The HF arc has a relatively small resistance, representing the lowest polarization contribution at any tested temperature, and the best fitting was obtained for a depressed semicircle and not a Warburg-type impedance. This could be attributed to finite-length oxygen-ion diffusion[19,20] through the electrode, and ion-transfer between electrode and electrolyte (as demonstrated in ref 21), presumably in the pure LSFC top electrode, since the composite support may have highly ion-conducting paths toward the electrolyte (Figures 4 and 7). On the other hand, the LF arc makes a major contribution to total sample resistance, especially at the lowest temperatures, and could be ascribed to the catalytic charge-transfer processes taking place on the electrode surface[21] and gas transport limitations[19] on both electrodes, which are especially critical at low temperatures and in the thick electrode with a much lower surface area available for oxygen reduction.

The Arrhenius plot (Figure 9) displays the product of the temperature and area-specific resistance (ASR) for the electrolyte, both electrode contributions, and the complete cell. The activation energy of the conduction in the thin electrolyte is 0.44 eV, and thus somewhat lower than the values obtained[22] for very thick $Ce_{0.9}Gd_{0.1}O_{1.95}$ pellets (motional enthalpy of oxide ions ~0.63 eV). This effect might be related to the dense packing, the remaining layer strains and the relatively low sintering temperature with respect to most of the previous studies. The electrolyte presents interesting ASR values even at the low temperatures suitable for IT-SOFC applications (600−500 °C), whereas the electrode polarization is much higher at low temperatures but decreases strongly when the temperature approaches 510 °C. Moreover, the selected CGO stoichiometry exhibited the

(18) Ivers-Tiffee E. , Weber A., Schichlein H. In *Handbook of Fuel Cells*; Vielstich W., Lamm A., Gasteiger H. A., Eds.; John Wiley & Sons: Chichester, U.K., 2003; Vol. 2, p 587.
(19) Grunbaum, N.; Dessemond, L.; Fouletier, J.; Prado, F.; Caneiro, A. *Solid State Ionics* **2006**, *177*, 907.
(20) Adler, S. B. *Solid State Ionics* **1998**, *111*, 125.
(21) Baumann, F. S.; Fleig, J.; Habermeier, H.-U.; Maier, J. *Solid State Ionics* **2006**, *177*, 1071.
(22) Huang, K.; Feng, M.; Goodenough, J. B. *J. Am. Ceram. Soc.* **1998**, *81* (2), 357.

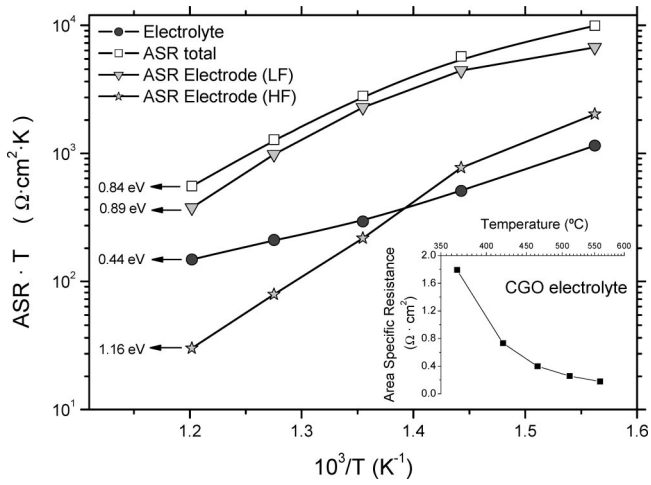

Figure 9. Arrhenius plot of the quasi-symmetric cell (shown in Figure 5) composed of (i) LSC-CGO (50:50 by weight percent) porous substrate (WE); (ii) a 20 μm thick CGO electrolyte; and (iii) a LSFC counter electrode. Area-specific resistance (and the related activation energy) of the CGO electrolyte, electrodes, and the whole cell as determined by EIS.

lowest (small-polaron) electronic conductivity under reducing conditions, the lowest grain boundary resistance and the highest oxygen ion conductivity.[29] In the inset of Figure 9, the electrolyte ASR is plotted directly against the temperature, showing a high ionic conductivity at temperatures as low as 460 °C. The activation energy of the HF and LF polarization is 1.16 eV and 0.89 eV, respectively. The addition of CGO to the macroporous LSC-based electrode (support) seems to reduce the apparent activation energy of the LF electrode polarization, which is typically around 1.3 eV for pure LSFC electrode and around 1.5−2.0 eV for pure LSC electrodes,[23–25] suggesting that the change in the mechanism limits the surface reactions, as previously reported in ref 26 and assuming that the macroporous electrode is determining the polarization steps. This limitation can be overcome by catalytically promoting the surface of the macroporous electrode by impregnation with precious metals, i.e., Pd, or nanoparticles of catalytic mixed oxides.[27]

A similar sample coated with a top anode (10 μm thick Pt layer) was measured under fuel cell operation conditions using air and wet diluted hydrogen as fuel at different temperatures: Figure 10 shows the DC electrochemical results. Figure 10a displays the evolution of the open current cell voltage (OCV) with the temperature for three different hydrogen concentrations. It can be observed that the OCV decreases gradually with increasing temperatures and decreasing hydrogen concentrations, i.e., increasing H_2O/H_2 ratios, as expected from a Nernstian behavior. However, the absolute cell potential is slightly lower than the theoretical Nernst value and this is ascribed to the (n-type) electronic conductivity of the CGO electrolyte. In fact, n-conductivity is strongly thermally activated under reducing conditions and it leads to intolerable leakage currents[28] at temperatures higher than 600 °C for the selected CGO stoichiometry.[29] OCV was constant during the measurement (5 min) and this is an indication that the (Pt) anode degradation is not observable under the applied operation conditions. Moreover, the obtained OCV values are lower than those observed by Ghosh et al.[1] in the same temperature range for a 20 μm thick $Ce_{0.8}Sm_{0.2}O_{1.9}$ (SDC) metal-supported cell. This mismatch could be directly attributed to (i) the use of the pure wet hydrogen as fuel in the cell testing and (ii) the use of a 2 μm thick dense $Zr_{0.82}Sc_{0.18}O_2$ (ScSZ) interlayer on the anode side, which acts as electronic insulator (pure oxygen-ion conductor), and therefore minimizing the internal short-circuit currents through the ScSZ |SDC electrolyte prepared by pulse laser deposition. Nevertheless the OCV values obtained here agree with (and are even higher than) those in refs 1 and 2, because they are based on the same system composition.

Figure 10b shows the DC polarization curves recorded in the temperature range 400−700 °C for a hydrogen concentration of 10%. The performance of the cell is in the same order of magnitude than previous reports based on the same configuration.[1,2] Differences in performance values can be explained by (i) the use of Pt anode limit the cell output due to the lack of oxygen ionic conductivity (TPB sites) and (ii) the use of diluted H_2 as fuel, notably increasing the anode polarization resistance. Indeed, the impedance measurements allow conclude that the major resistance contribution is given by the anode processes. The larger impedance values observed at low frequencies (with relaxation frequency ca. 3.5 Hz) are related to the Pt-anode processes, since the impedance value of this semicircle strongly increases with decreasing hydrogen contents (see Figure S6 in the Supporting Information). Nevertheless, the contribution of the cathode processes is still important and should be improved by promoting the surface of the macroporous substrate with electrocatalytic species based on the Ba−Pr ferrites and cobaltites.[30–32] The apparent activation energy of the cell with the Pt-anode was calculated from the polarization curves at 0.55 V and has a constant value of 0.57 eV for the whole temperature range.

Finally, a mixed conducting thin layer composed of LSFC was tested for oxygen separation from air using helium as the sweep gas in the range of 650−1000 °C. This sample consists of a 10 μm thick gastight LSFC layer supported on a porous LSFC-CGO composite (cross-section shown in Figure 2c). The permeation results are displayed in Figure 11, showing the Arrhenius plot of the oxygen flux against the inverse of the temperature. After sealing, a ration O_2 to N_2 higher than 25 was observed in the permeate stream. The flux obtained for a 1 mm thick gastight LSFC membrane is introduced in order to highlight the considerable improvement (5-fold) of the flux obtained by decreasing the thickness

(23) Bueberle-Hütter, A.; Søgaard, M.; Tuller, H. L. *Solid State Ionics* **2006**, *177*, 1969.
(24) Yasumoto, K.; Inagaki, Y.; Shiono, M.; Dokiya, M. *Solid State Ionics* **2002**, *148*, 545.
(25) Srdic, V. V.; Omorjan, R. P.; Seydel, J. *Mater. Sci. Eng.* **2005**, *116*, 119.
(26) Perry Murray, E.; Server, M. J.; Barnett, S. A. *Solid State Ionics* **2002**, *148*, 27.
(27) Sholklapper, T. Z.; Kurokawa, H.; Jacobson, C. P.; Visco, S. J.; De Jonghe, L. C. *Nano Lett.* **2007**, *7*, 2136.
(28) Miyashita, T. *J. Mater. Sci.* **2006**, *41*, 3183.
(29) Haile, S. M. *Acta Mater.* **2003**, *51*, 5981.
(30) Serra, J. M.; Buchkremer, H.-P. *J. Power Sources* **2007**, *172*, 768.
(31) Shao, Z.; Haile, S. M. *Nature* **2004**, *431*, 170.
(32) Liu, Q. L.; Khor, K. A.; Chan, S. H. *J. Power Sources* **2006**, *161*, 123.

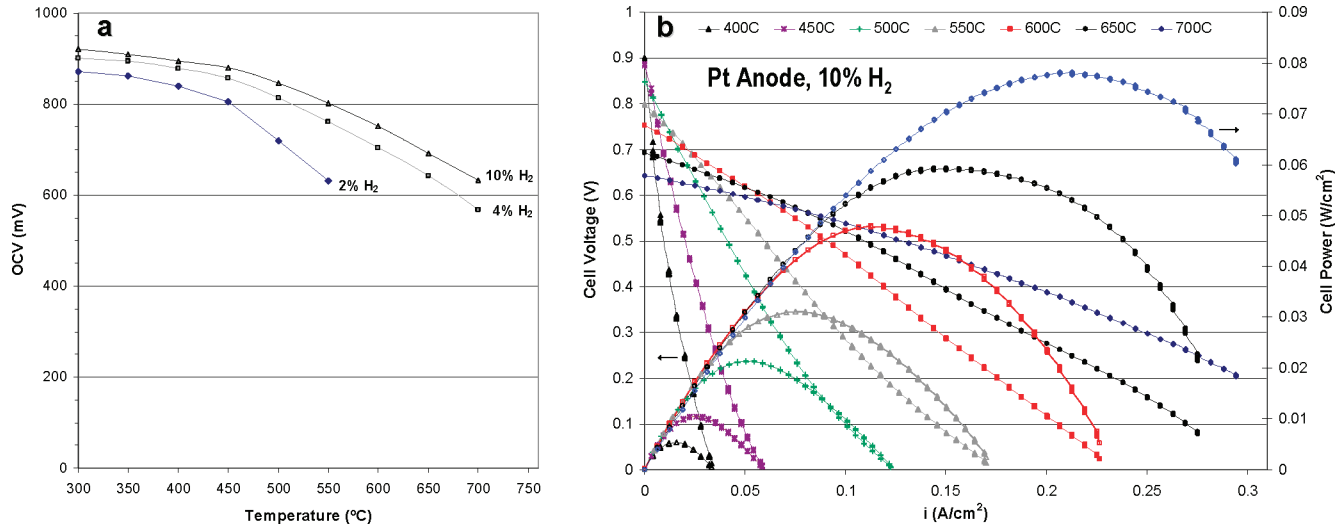

Figure 10. Fuel cell electrochemical characterization using hydrogen diluted with nitrogen and saturated with water at 25 °C as fuel and air: (a) open current voltage as a function of the operating temperature and the hydrogen LSC-CGO (50:50 by weight percent) porous substrate (cathode); (ii) a 20 μm thick CGO electrolyte; and (iii) a 10 μm thick porous Pt anode; and (b) cell voltage vs current density polarization curves at 10% hydrogen as a function of the temperature.

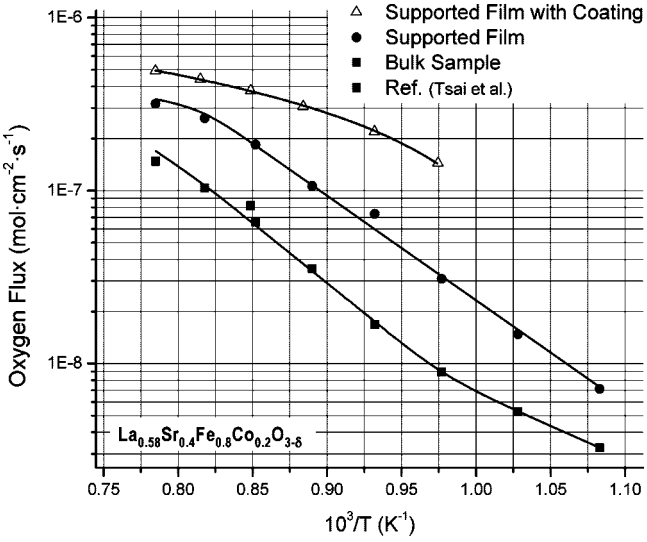

Figure 11. Oxygen permeation flux of two LSFC membranes: one bulk sample (1 mm thickness) and a thin film (~10 μm thickness) supported on a LSFC-CGO (70:30 by weight percent) composite substrate. Air supplied with 100 mL/min air and sweep side with 150 mL/min helium. Sealing carried out using a gold seal at 1020 °C. Referenced permeation values from ref 35.

(~75 times smaller). Nevertheless, the lack of linear correlation between decreasing thickness and oxygen flux is a sign of the change in the rate-determining mechanism of the oxygen permeation. Indeed, the thin-layer permeation may be presumably controlled by the surface exchange processes while the limiting step for the bulk membrane may be oxygen ion transport through the membrane. However, this point cannot be clarified by comparing the activation energy of both samples in the most linear temperature range. The activation energy of the LSFC bulk membrane is 1.38 eV while for the supported thin film it is 1.20 eV. The two values do not differ much in this case and are in reasonable agreement with previous studies on this ferrite composition using isotopic exchange techniques.[33] Other materials, like $Ba_{0.5}Sr_{0.5}Fe_{0.2}Co_{0.8}O_{3-\delta}$ (BSFC), with a similar stoichiometry may exhibit a clear difference[31] in activation energy, i.e., bulk (0.44 eV) and oxygen exchange (1.2 eV). Further improvement to the permeation rate was achieved by applying a catalytic porous coating on the top surface of the supported film. The selected catalyst composition comprises $Pr_{0.58}Sr_{0.4}Fe_{0.8}Co_{0.2}O_{3-\delta}$ impregnated with Pd nitrate (Pd 1% wt.), due to its high electrocatalytic activity as SOFC cathode.[34] The obtained permeation rate implies an improvement with respect to the bulk sample of more than 1 order of magnitude at 750 °C and a 6-fold improvement with respect to the nonactivated supported thin film. In this case, the observed activation energy does change for the coated thin film and is reduced to 0.55 eV. In fact, it is visible that the permeation through this membrane is much less thermally activated at temperatures higher than 800 °C, and it seems that there is a change in the rate determining step (activation energy), approaching the behavior of the other two membranes at lower temperatures. Surprisingly, this activation energy is similar to the apparent activation energy observed for the SOFC operation with this same catalytic coating as cathode.[34] Nevertheless, higher oxygen fluxes have been obtained using other membrane compositions, i.e., BSFC, although these highly permeable materials exhibit very low chemical stability at low oxygen partial pressure, high reactivity with CO_2, and very pronounced chemical expansion behavior.

4. Conclusions. Cathode-supported fuel cells with a 10 μm thick $Ce_{0.8}Gd_{0.2}O_{1.9}$ electrolyte were prepared and tested, and exhibited a great potential for operation in the temperature range of 500−600 °C. The area specific resistance of the CGO electrolyte is very low (250 mΩ cm^2 at 550 °C), whereas the cathode polarization is acceptable although it should be further improved. On the other hand, oxygen-permeable membranes were prepared using the same procedure. A 10 μm thick $La_{0.58}Sr_{0.4}Fe_{0.8}Co_{0.2}O_{3-\delta}$ gastight layer

(33) Esquirol, A.; Kilner, J.; Brandon, N. *Solid State Ionics* **2004**, *175*, 63.
(34) Serra, J. M.; Vert, V. B.; Betz, M.; Haanappel, V. A. C.; Meulenberg, W. A.; Tietz, F. *J. Electrochem. Soc.* **2008**, *155*, B207.
(35) Tsai, C. Y.; Dixon, A. G.; Ma, Y. H.; Moser, W. R.; Pascucci, M. R. *J. Am. Ceram. Soc.* **1998**, *81*, 1437.

supported on a composite ($La_{0.58}Sr_{0.4}Fe_{0.8}Co_{0.2}O_{3-\delta}$-CGO 70:30 by weight percent) with a catalytic coating showed an oxygen flux 1 order of magnitude higher than the one obtained for a thick $La_{0.58}Sr_{0.4}Fe_{0.8}Co_{0.2}O_{3-\delta}$ membrane. This kind of membranes is promising for efficient oxygen separation, especially if the surface oxygen exchange and the resistance to carbonation are improved.

The use of tailored MIEC composites composed of LSFC and CGO as porous substrates permitted the thermal expansion and chemical compatibility to be adjusted with respect to the top oxygen conducting layers. The optimization of the most relevant composite properties enabled a gastight thin electrolyte/membrane to be obtained using inexpensive preparation techniques, such as screen-printing or slip-casting. The SOFCs thus obtained showed good connectivity between grains of cathode, anode and electrolyte. Moreover, the sintering temperature required to achieve gas tightness was reduced, while retaining a relatively high porosity and surface area, and as a result, the electrocatalytic activity for oxygen exchange was not notably diminished.

Acknowledgment. Financial support by the Fundación Ramón Areces, the Universitat Politècnica de València (Grant UPV-2007-06), and the Helmholtz Association of German Research Centers through the Helmholtz Alliance MEM-BRAIN (Initiative and Networking Fund) is kindly acknowledged. The authors thank M D. Sebold and E. Wessel for SEM analysis, and U. Breuer for SIMS analysis. F. Wiener and S. Escolástico contributed to this work by performing the oxygen permeation experiments. Mrs. J. Carter-Sigglow has contributed to this work with her careful revision of the English usage.

Supporting Information Available: Additional SEM images, EDS microanalysis, photographs of samples, electrical conductivity, impedance measurement of a fully assembled fuel cell, and flow resistances measurements through the porous substrates (PDF). This material is available free of charge via the Internet at http://pubs.acs.org.

CM702508F